

Valley separation in graphene by polarized light

L. E. Golub and S. A. Tarasenko*

*Ioffe Physical-Technical Institute of the RAS, RU-194021 St. Petersburg, Russia*M. V. Entin¹ and L. I. Magarill^{1,2}¹*Institute of Semiconductor Physics, Siberian Branch of the RAS, RU-630090 Novosibirsk, Russia*²*Novosibirsk State University, RU-630090 Novosibirsk, Russia*

(Received 10 October 2011; published 2 November 2011)

We show that the optical excitation of graphene with polarized light leads to pure valley current for which carriers in the valleys counterflow. The current in each valley originates from the asymmetry of optical transitions and electron scattering by impurities owing to the warping of the electron energy spectrum. The valley current has strong polarization dependence; its direction is opposite for normally incident beams of orthogonal linear polarizations. In undoped graphene on a substrate with high susceptibility, electron-electron scattering leads to an additional contribution to the valley current that can dominate.

DOI: [10.1103/PhysRevB.84.195408](https://doi.org/10.1103/PhysRevB.84.195408)

PACS number(s): 78.67.Wj, 72.80.Vp, 73.50.Pz

I. INTRODUCTION

Graphene, a one-atom-thick layer of carbon with a honeycomb crystal lattice, has been attracting rapidly growing attention due to its unique electronic properties. Its zero band gap and zero effective-electron and -hole masses as well as its high mobility make it interesting for both fundamental and applied research.¹⁻³ The electron excitations in graphene are similar to massless Dirac fermions with their cone points situated at the points K and K' of the Brillouin zone. The interplay of two equivalent valleys gives rise to new transport and optical phenomena that are absent in systems with simple electron dispersion and underlies the novel research field called “valleytronics.”^{4,5} In multivalley structures, one can independently control the carriers in different valleys⁶ and construct peculiar electron distributions in which particles in the valleys flow predominantly in different directions.⁷

Previous research on the valley-dependent transport in graphene has focused on the manipulation of charge carriers by static electric fields. It was demonstrated that the electric field may induce valley-polarized current in a graphene point contact with zigzag edges,⁵ a graphene layer with broken inversion symmetry,⁸ at the boundary between monolayer and bilayer graphene,⁹ and at a line defect¹⁰ as well as in the case in which monolayer or bilayer graphene is additionally illuminated by circularly polarized radiation.^{11,12} It was also proposed in Ref. 13 that valley currents can be induced in mesoscopic graphene rings by asymmetrical monocycle electromagnetic pulses. Here, we show that valley separation can be achieved in a homogeneous graphene layer by purely optical means. We demonstrate that the interband excitation of graphene by linearly polarized light leads to the electron current in each valley, the direction of which is determined by the light polarization. The partial photocurrents $j^{(v)}$ ($v = \pm$ for the valleys K and K' , respectively) in the ideal honeycomb structure are directed opposite to one another so that the total electric current $\mathbf{j}^{(+)} + \mathbf{j}^{(-)}$ vanishes. We also briefly discuss the optical and transport methods to reveal the pure valley current.

Phenomenologically, the emergence of the valley photocurrent is related to the low point-group symmetry of the

individual valleys. Despite the fact that the crystal lattice of flat graphene is centrosymmetric, the valleys K and K' are described by the wave-vector group D_{3h} , lacking space inversion (see Fig. 1). The group D_{3h} allows for the photocurrent induced by normally incident, linearly polarized light. Symmetry analysis shows that the polarization dependences of the current components in the valley K are given by

$$j_x^{(+)} = \chi(e_x^2 - e_y^2)I, \quad j_y^{(+)} = -2\chi e_x e_y I. \quad (1)$$

Here, χ is a parameter, e_x and e_y are components of the (real) light-polarization unit vector \mathbf{e} , I is the intensity of the incident light, and the x axis is chosen along the Γ - K line [see Fig. 1(a)]. The photocurrent in the valley K' is obtained by the replacement $x \rightarrow -x$ on both sides of Eq. (1), giving $\mathbf{j}^{(-)} = -\mathbf{j}^{(+)}$. We note that the absence of a total electric current at a normal incidence of radiation is in agreement with the symmetry arguments allowing for a photocurrent in noncentrosymmetric systems only. At an oblique incidence of radiation, a net current in graphene may arise due to the photon-drag effect caused by the transfer of phonon linear momenta to free carriers.^{14,15}

II. MICROSCOPIC THEORY

The microscopic model of pure-valley-current generation is based on the trigonal warping of the energy spectrum of carriers in the valleys. The effective Hamiltonian describing electron and hole states in the vicinity of the K and K' points has the form¹⁶

$$\hat{H}_p^{(v)} = \begin{pmatrix} 0 & \Omega_p^{(v)} \\ \Omega_p^{(v)*} & 0 \end{pmatrix}. \quad (2)$$

Here, \mathbf{p} is the momentum counted from the valley center,

$$\Omega_p^{(v)} = v v_0 (p_x - i p_y) - \mu (p_x + i p_y)^2, \quad (3)$$

where v_0 is the electron velocity and μ is the parameter of the warping that reflects the trigonal symmetry of the valleys (D_{3h} wave-vector group). In the framework of the tight-binding model, $\mu = v_0 a / (4\sqrt{3}\hbar)$ with a being the lattice constant.² We assume that the warping is small and, therefore, calculate

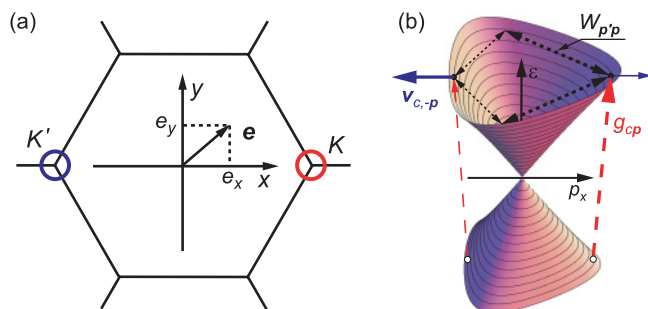


FIG. 1. (Color online) (a) Brillouin zone of graphene. The circles indicate the neighborhood of the K and K' points in which the electron states have trigonal symmetry allowing for the photocurrent. (b) Mechanisms of photocurrent formation in the K valley. Solid, dashed, and dotted arrows of different thicknesses indicate anisotropy of velocity, optical generation, and scattering rate, respectively, in \mathbf{p} space.

the current to the first order in μ . The energy spectrum of the carriers in the conduction c and valence v bands is given by

$$\varepsilon_{cp}^{(v)} \approx v_0 p - v\mu p^2 \cos 3\varphi_p, \quad \varepsilon_{vp}^{(v)} = -\varepsilon_{cp}^{(v)}, \quad (4)$$

where φ_p is the polar angle of the momentum \mathbf{p} .

Figure 1(b) shows the energy spectrum in the K valley with the warping included. The inequality of $\varepsilon_{cp}^{(+)}$ and $\varepsilon_{c,-p}^{(+)}$ (as well as that of $\varepsilon_{vp}^{(+)}$ and $\varepsilon_{v,-p}^{(+)}$) gives rise to an electric current in the valley if electrons are optically excited from the valence to the conduction band by linearly polarized light. In the valley K' , the warping of the energy spectrum is opposite [Eq. (4)], and the photocurrent direction is reversed.

In the framework of kinetic theory, the photocurrent densities in the valleys are given by

$$\mathbf{j}^{(v)} = 2e \sum_{\mathbf{p}} (\mathbf{v}_{c\mathbf{p}}^{(v)} f_{c\mathbf{p}}^{(v)} + \mathbf{v}_{v\mathbf{p}}^{(v)} f_{v\mathbf{p}}^{(v)}), \quad (5)$$

where e is the electron charge, the factor 2 accounts for the spin degeneracy, $\mathbf{v}_{c,v}^{(v)} = \nabla_{\mathbf{p}} \varepsilon_{c,v}^{(v)}$ are the velocities, and $f_{c\mathbf{p}}^{(v)}$ and $f_{v\mathbf{p}}^{(v)}$ are the nonequilibrium corrections to the distribution functions in the conduction and valence bands linear in the light intensity, respectively. $f_{c\mathbf{p}}^{(+)} = f_{c,-\mathbf{p}}^{(-)}$ and $f_{v\mathbf{p}}^{(+)} = f_{v,-\mathbf{p}}^{(-)}$ due to space inversion symmetry. We consider interband optical transitions in undoped graphene at low temperatures. Owing to electron-hole symmetry, $f_{c\mathbf{p}}^{(v)} = -f_{v\mathbf{p}}^{(v)}$, and the photocurrent [Eq. (5)] assumes the form $\mathbf{j}^{(v)} = 4e \sum_{\mathbf{p}} \mathbf{v}_{c\mathbf{p}}^{(v)} f_{c\mathbf{p}}^{(v)}$.

The steady-state correction to the distribution function can be found from the kinetic equation

$$\sum_{\mathbf{p}'} (W_{\mathbf{p}\mathbf{p}'}^{(v)} f_{c\mathbf{p}'}^{(v)} - W_{\mathbf{p}'\mathbf{p}}^{(v)} f_{c\mathbf{p}}^{(v)}) + \text{St}^{(ee)} + g_{c\mathbf{p}}^{(v)} = 0, \quad (6)$$

where $W_{\mathbf{p}\mathbf{p}'}^{(v)}$ is the rate of intravalley electron scattering by static defects or impurities, the weak intervalley processes are neglected, $g_{c\mathbf{p}}^{(v)}$ is the optical generation rate, and $\text{St}^{(ee)}$ describes electron-electron collisions.

First, we consider the valley current in the presence of intensive electron scattering by impurities and neglect

electron-electron collisions. We focus on the photocurrent in the K valley and omit index $\nu = +$. In the Born approximation, the rate of elastic electron scattering by impurities $W_{\mathbf{p}\mathbf{p}'} = W_{\mathbf{p}'\mathbf{p}}$ is given by

$$W_{\mathbf{p}\mathbf{p}'} = \frac{\pi}{2\hbar} \left| 1 + \frac{\Omega_{\mathbf{p}} \Omega_{\mathbf{p}'}^*}{|\Omega_{\mathbf{p}} \Omega_{\mathbf{p}'}|} \right|^2 \mathcal{K}(|\mathbf{p}' - \mathbf{p}|) \delta(\varepsilon_{c\mathbf{p}} - \varepsilon_{c\mathbf{p}'}), \quad (7)$$

where $\mathcal{K}(q)$ is the Fourier component of the impurity-potential correlator. The specific angular dependence of $W_{\mathbf{p}\mathbf{p}'}$ follows from the Hamiltonian of Eq. (2). The generation rate in the conduction band $g_{c\mathbf{p}}$ is determined by the interband matrix elements of the velocity operator $\nabla_{\mathbf{p}} \hat{H}_{\mathbf{p}}$. In the regime linear in the radiation intensity, it has the form

$$g_{c\mathbf{p}} = \frac{2\pi}{\hbar} \left(\frac{eA}{c} \right)^2 \left| \text{Im} \left(\frac{\Omega_{\mathbf{p}}^*}{|\Omega_{\mathbf{p}}|} \mathbf{e} \cdot \nabla_{\mathbf{p}} \Omega_{\mathbf{p}} \right) \right|^2 \delta(\hbar\omega - 2\varepsilon_{c\mathbf{p}}). \quad (8)$$

Here, ω is the light frequency, $A/2$ is the amplitude of the vector potential of the electromagnetic wave, related to the intensity of the incident light by $I = A^2 \omega^2 / (2\pi c t_0^2)$, and t_0 is the amplitude-transmission coefficient; $t_0 = 2/(n+1)$ for graphene on a substrate with the refractive index n .

As follows from Eqs. (5) and (6), the valley current arises due to warping-induced asymmetry in the electron velocity $\mathbf{v}_{c\mathbf{p}}$, the scattering rate $W_{\mathbf{p}\mathbf{p}'}$, and the generation rate $g_{c\mathbf{p}}$. Accordingly, to the first order in μ , one can distinguish three contributions to the current Eq. (1), $\chi = \chi^{(\text{vel})} + \chi^{(\text{gen})} + \chi^{(\text{sc})}$. The corresponding mechanisms of the current formation are sketched in Fig. 1(b).

To calculate the valley current caused by the velocity correction, one neglects the warping in the optical-generation and scattering rates. In this mechanism, the absorption of linearly polarized light leads to the alignment of electron momenta described by the second angular harmonic of the distribution function.¹⁷ Owing to the μ -linear correction to the velocity, such a distribution of carriers in \mathbf{p} space implies an electric current [Eq. (1)] with

$$\chi^{(\text{vel})} = \frac{5e\mu\eta\tau_2(\varepsilon_\omega)t_0^2}{8v_0}. \quad (9)$$

Here, $\varepsilon_\omega = \hbar\omega/2$ is the kinetic energy of photoelectrons, τ_n ($n = 1, 2, \dots$) are the relaxation times of the n th angular harmonics of the distribution function, $\tau_n^{-1} = \sum_{\mathbf{p}'} W_{\mathbf{p}\mathbf{p}'} (1 - \cos n\theta)$, θ is the angle between \mathbf{p} and \mathbf{p}' , and $\eta = \pi e^2 / \hbar c$ is the absorbance³ for normally incident light.

Another contribution to the valley current comes from the asymmetry of photoexcitation. Indeed, to the first order in μ , the optical-generation rate $g_{c\mathbf{p}}$ contains the first angular harmonic, which gives rise to a photocurrent

$$\chi^{(\text{gen})} = -\frac{e\mu\eta t_0^2}{8v_0} \left[9\tau_1(\varepsilon_\omega) + \varepsilon_\omega \frac{d\tau_1(\varepsilon_\omega)}{d\varepsilon_\omega} \right]. \quad (10)$$

The third mechanism of the current generation originates from the asymmetry of photoelectron scattering. The solution $f_{c\mathbf{p}}$ of kinetic Eq. (6) contains the first angular harmonic even if the warping is neglected in the optical-generation rate of Eq. (8) but taken into account in the scattering rate of Eq. (7). Such a contribution to the valley current is

given by

$$\chi^{(\text{sc})} = \frac{e\mu\eta\tau_2 t_0^2}{8v_0} \left\{ 20 - 6\frac{\tau_1}{\tau_2} - 4\frac{\tau_1}{\tau_3} + \frac{\varepsilon_\omega}{2} \left[\left(\frac{9}{\tau_1} - \frac{2}{\tau_2} \right) \frac{d\tau_1}{d\varepsilon_\omega} + \tau_1 \frac{d}{d\varepsilon_\omega} \left(\frac{1}{\tau_2} + \frac{1}{\tau_3} \right) \right] \right\}, \quad (11)$$

where the relaxation times are taken at the energy ε_ω .

Equations (9)–(11) demonstrate that both the magnitude and excitation spectrum of the pure valley current are determined by the mechanisms of scattering. For electron scattering by unscreened Coulomb impurities in graphene, one obtains $\tau_1 \propto \varepsilon$, $\tau_2 = 3\tau_1$, and $\tau_3 = 5\tau_1$. Such relations yield $\chi \propto \omega$. In the case of scattering by short-range static defects, one has $\tau_1 \propto 1/\varepsilon$, $\tau_2 = \tau_3 = \tau_1/2$, and therefore $\chi \propto 1/\omega$. Estimation shows the valley currents in suspended graphene $j^{(\pm)} \sim 10^{-4}$ A/cm at the light intensity $I = 1$ W/cm², $\tau_1 = 10^{-12}$ s,³ $\mu = 3.6 \times 10^{26}$ g⁻¹, and $v_0 = 10^8$ cm/s.

III. EFFECT OF ELECTRON-ELECTRON SCATTERING

Now, we analyze the effect of electron-electron interaction on the pure valley current. It is well known that in systems with parabolic energy spectra, the interparticle collisions partially suppress the anisotropy of the distribution functions. Therefore, one can expect that electron-electron scattering (between carriers from the same valley and, in particular, between carriers from different valleys) can only decrease the pure valley current. We demonstrate below that the interparticle collisions in graphene may give rise to an additional contribution to the valley photocurrent.

Consider the collision of a photoelectron with momentum \mathbf{p} from the valley ν of the conduction band with an electron with momentum \mathbf{k} from the valley ν' of the valence band. After the collision, both electrons reside in the conduction

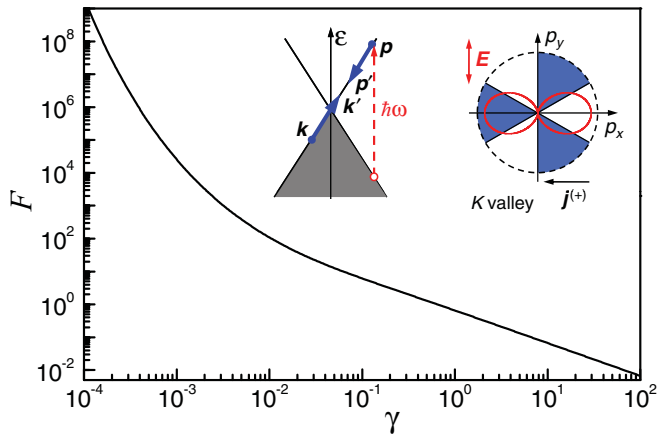


FIG. 2. (Color online) Dependence $F(\gamma)$ that determines the magnitude of the valley current caused by electron-electron scattering [Eq. (17)]. The left inset sketches the scattering of electrons with momenta \mathbf{p} and \mathbf{k} into states with momenta \mathbf{p}' and \mathbf{k}' , respectively. The right inset shows the momentum space in the K valley. Sectors where the Auger-like electron relaxation is allowed are colored, and the ellipses depict the alignment of the photoelectron momenta by linearly polarized light.

band with momenta \mathbf{p}' and \mathbf{k}' , respectively (see the left inset of Fig. 2). Processes of other kinds are negligible in undoped graphene at low temperatures and weak excitation levels. The Coulomb interaction between carriers leads to the transfer of momentum $q \sim \omega/v_0 \ll \pi/a$, therefore, both electrons remain in the valleys where they were before the collision although the valleys ν and ν' may be different. The momentum and energy conservation laws read

$$\mathbf{p} + \mathbf{k} = \mathbf{p}' + \mathbf{k}', \quad \varepsilon_{c\mathbf{p}}^{(\nu)} + \varepsilon_{v\mathbf{k}}^{(\nu')} = \varepsilon_{c\mathbf{p}'}^{(\nu)} + \varepsilon_{c\mathbf{k}'}^{(\nu')}. \quad (12)$$

In the conic approximation, Eq. (12) implies that $k < p$, $p' + k' < p$, and \mathbf{k} should be antiparallel while \mathbf{p}' and \mathbf{k}' are parallel to \mathbf{p} .¹⁸ The possibility of the collisions is determined by corrections to the linear dispersion. Interaction-induced renormalization of the energy spectrum makes it concave,^{19,20} forbidding such Auger-like processes. On the other hand, the spectrum warping does allow for these processes. In graphene on a substrate with high susceptibility, the interaction effects are suppressed, and the warping becomes prevailing. An estimation shows that for an electron with energy $\varepsilon = 0.3$ eV, this regime occurs at the effective dielectric constant $\varepsilon^* > 300$. Besides, interaction effects can be suppressed by a metallic gate or by increasing the temperature. Neglecting the interaction-induced renormalization of the energy spectrum, we obtain from Eq. (12) to the first order in μ :

$$v_0(pk\alpha^2 + p'k'\beta^2) = -2\mu\nu(p-p')(p'+k')[p+p'+\nu\nu'(k-k')] \cos 3\varphi_p, \quad (13)$$

where $\alpha = \varphi_p - \pi - \varphi_k \ll 1$ and $\beta = \varphi_{k'} - \varphi_{p'} \ll 1$. Equation (13) has solutions only for sectors of φ_p where the second line is positive, i.e., for $\mu\nu \cos 3\varphi_p < 0$, meaning that Auger-like processes for electrons with momentum \mathbf{p} are allowed or forbidden depending on the sign of $\cos 3\varphi_p$ (see the right inset of Fig. 2).

The angular dependence of the electron-electron collision rate in graphene gives rise to a pure valley current if the sample is illuminated by linearly polarized light. The mechanism of the current generation is sketched in the right inset of Fig. 2. The absorption of linearly polarized light leads to the alignment of electron momenta described by the second angular harmonic of the distribution function. The photoexcited electrons are scattered by resident electrons from the valence band and lose their energies. Since the scattering rate is anisotropic, the energy relaxation leads to the formation of the first harmonic of the distribution function and to an electric current if the momentum relaxation time depends on energy. In the case of weak electron-electron scattering ($\tau_{ee} \gg \tau_1$, where τ_{ee} is the electron-electron scattering time), the mechanism efficiency can be estimated as $\chi^{(\text{ee})} \sim e\nu_0\eta\tau_1^2/(\varepsilon_\omega\tau_{ee})$.

To calculate the pure valley current caused by electron-electron scattering, we solve the kinetic Eq. (6) with the linearized collision integral:

$$\text{St}^{(\text{ee})} = \frac{4\pi}{\hbar} \sum_{\mathbf{k}, \mathbf{k}', \mathbf{p}', \mathbf{v}'} |u_{\mathbf{p}-\mathbf{p}'}|^2 \delta_{\mathbf{p}+\mathbf{k}, \mathbf{p}'+\mathbf{k}'} \left\{ [f_{c\mathbf{p}'}^{(\nu)} \delta(\varepsilon_{c\mathbf{p}}^{(\nu)} + \varepsilon_{c\mathbf{k}}^{(\nu')} - \varepsilon_{c\mathbf{p}'}^{(\nu)} - \varepsilon_{v\mathbf{k}'}^{(\nu')}) - (\mathbf{p} \leftrightarrow \mathbf{p}')] + [f_{c\mathbf{k}'}^{(\nu')} \delta(\varepsilon_{c\mathbf{p}}^{(\nu)} + \varepsilon_{c\mathbf{k}}^{(\nu')} - \varepsilon_{v\mathbf{p}'}^{(\nu)} - \varepsilon_{c\mathbf{k}'}^{(\nu')}) + (\mathbf{k} \leftrightarrow \mathbf{k}')] \right\}, \quad (14)$$

where $u_q = 2\pi\hbar e^2/(\epsilon^*q)$ is the Fourier component of the Coulomb potential and the factor 4 accounts for the spin degeneracy. In Eq. (14), we assume that the warping is small and take it into account only in the arguments of δ functions. The consequent simplification of $\text{St}^{(\text{ee})}$ consists in summing over the almost collinear momenta. Kinetic Eq. (6) with the simplified electron-impurity-collision term $-f_{c\mathbf{p}}^{(v)}/\tau$ takes the form

$$g_{c\mathbf{p}} = -\frac{\pi e^4}{\hbar^3 v_0 \epsilon^{*2} p} \left[\int_p^\infty dk (\sqrt{k} - \sqrt{p})^2 (f_{c\mathbf{k}}^{(+)} + f_{c\mathbf{k}}^{(-)}) + \theta(-v \cos 3\varphi_p) \left(\int_p^\infty dk \frac{\sqrt{kp}}{2} f_{c\mathbf{k}}^{(v)} - \frac{p^2}{3} f_{c\mathbf{p}}^{(v)} \right) \right] + \frac{f_{c\mathbf{p}}^{(v)}}{\tau}, \quad (15)$$

where $\varphi_{\mathbf{k}} = \varphi_{\mathbf{p}}$ and $\theta(x)$ is the Heaviside step function. In the case of $1/\tau(\epsilon) = 2\pi^2 e^4 N_i / (\hbar \epsilon^{*2} \epsilon)$, which corresponds to the momentum relaxation time of electrons due to scattering by Coulomb impurities with surface density N_i , Eq. (15) can be transformed into the differential equation

$$\gamma u(u^4 + 6\gamma)J''''(u) + \gamma(5u^4 - 16\gamma)J'''(u) + 2u^2(u^4 + 12\gamma)J'(u) + 12u(u^4 - 2\gamma)J(u) = 0 \quad (16)$$

for the function

$$J(u) = \frac{\epsilon_\omega^2 \int_0^{2\pi} f_{c\mathbf{p}}^{(+)} \theta(\cos 3\varphi_p) \cos \varphi_p d\varphi_p}{2\pi^2 v_0^2 \tau(\epsilon_\omega) \sum_p g_{c\mathbf{p}} \theta(\cos 3\varphi_p) \cos \varphi_p} - \delta(u - 1).$$

Here, $u = \sqrt{v_0 p / \epsilon_\omega}$, $J'(u) = dJ(u)/du$, and the parameter $\gamma = \pi N_i \hbar^2 v_0^2 / \epsilon_\omega^2$ characterizes the rate of electron scattering by impurities with respect to the electron-electron scattering rate. $J(u)$ satisfies the boundary conditions $J(1) = J'(1) = 0$, $J''(1) = 2(1 + 12\gamma)/[\gamma(1 + 6\gamma)]$, and $J'''(1) = -36/(1 + 6\gamma)^2$. Finally, the contribution to the valley current induced by electron-electron scattering is given by Eq. (1) with

$$\chi^{(\text{ee})} = -\frac{e v_0 \eta \tau(\epsilon_\omega) t_0^2}{4\pi \epsilon_\omega} F(\gamma), \quad (17)$$

where $F(\gamma) = \int_0^1 J(u) u^3 du - \gamma J(0)/2 + 1$. The function $F(\gamma)$ also determines the excitation spectrum of the valley

current since $\gamma \propto 1/\omega^2$. $F(\gamma)$ calculated numerically from Eq. (16) is shown in Fig. 2. The estimation for $\hbar\omega = 1$ eV and $N_i = 10^{12} \text{ cm}^{-2}$ yields $\gamma \sim 10^{-2}$ and $\chi^{(\text{ee})}$ being two orders of magnitude larger than $\chi^{(\text{vel})}$. Thus, for graphene on a substrate with high susceptibility, the mechanism of valley-current formation caused by electron-electron scattering dominates.

IV. SUMMARY

To summarize, we have shown that the homogeneous excitation of graphene with linearly polarized light results in a pure valley current. We have developed a microscopic theory of this effect and demonstrated that the valley current has specific polarization dependence. Pure valley current is not accompanied by any net-charge current but leads to the accumulation of valley-polarized carriers at edges of the sample. The valley polarization breaks the time-inversion symmetry and also implies the local lowering of the space symmetry to the D_{3h} group of a single valley, which lacks space inversion. Such a lowering of the space symmetry can be detected by optical means, e.g., by a second-harmonic generation of the probe beam.

Another possibility to register the valley current is to convert it into an electric current. It can be realized, e.g., in curved graphene. The curvature of the graphene sheet produces effective out-of-plane magnetic fields that are directed oppositely for electrons in the valleys K and K' .²¹ Owing to the Lorentz force, the magnetic fields change the directions of the partial currents in the valleys, giving rise to a measurable net electric current. Straightforward estimation shows that the net electric current $\mathbf{j}^{(+)} + \mathbf{j}^{(-)} \sim [\mathbf{j}^{(+)} \times \boldsymbol{\omega}_c^*] \tau$, provided the cyclotron frequency of the effective field ω_c^* is smaller than the momentum-scattering rate.

ACKNOWLEDGMENTS

We thank E. L. Ivchenko, D. L. Shepelyansky, and A. D. Chepelianskii for stimulating discussions. This work was supported by the Russian Foundation for Basic Research, a President grant for young scientists, and the Dynasty Foundation affiliated with the International Center for Fundamental Physics in Moscow.

*tarasenko@coherent.ioffe.ru

¹A. K. Geim and K. S. Novoselov, *Nat. Mater.* **6**, 183 (2007).
²A. H. Castro Neto, F. Guinea, N. M. R. Peres, K. S. Novoselov, and A. K. Geim, *Rev. Mod. Phys.* **81**, 109 (2009).
³N. M. R. Peres, *Rev. Mod. Phys.* **82**, 2673 (2010).
⁴S. A. Tarasenko and E. L. Ivchenko, *Pis'ma Zh. Eksp. Teor. Fiz.* **81**, 292 (2005) [*JETP Lett.* **81**, 231 (2005)].
⁵A. Rycerz, J. Tworzydło, and C. W. J. Beenakker, *Nat. Phys.* **3**, 172 (2007).
⁶A. A. Kaplyanskiy, N. S. Sokolov, B. V. Novikov, and S. V. Gastev, *Solid State Commun.* **20**, 27 (1976).
⁷J. Karch, S. A. Tarasenko, E. L. Ivchenko, J. Kamann, P. Olbrich, M. Utz, Z. D. Kvon, and S. D. Ganichev, *Phys. Rev. B* **83**, 121312 (2011).

⁸D. Xiao, W. Yao, and Q. Niu, *Phys. Rev. Lett.* **99**, 236809 (2007).
⁹T. Nakanishi, M. Koshino, and T. Ando, *Phys. Rev. B* **82**, 125428 (2010).
¹⁰D. Gunlycke and C. T. White, *Phys. Rev. Lett.* **106**, 136806 (2011).
¹¹T. Oka and H. Aoki, *Phys. Rev. B* **79**, 081406 (2009).
¹²D. S. L. Abergel and T. Chakraborty, *Appl. Phys. Lett.* **95**, 062107 (2009).
¹³A. S. Moskalenko and J. Berakdar, *Phys. Rev. B* **80**, 193407 (2009).
¹⁴M. V. Entin, L. I. Magarill, and D. L. Shepelyansky, *Phys. Rev. B* **81**, 165441 (2010).
¹⁵J. Karch, P. Olbrich, M. Schmalzbauer, C. Zoth, C. Brinsteiner, M. Fehrenbacher, U. Wurstbauer, M. M. Glazov, S. A. Tarasenko, E. L. Ivchenko, D. Weiss, J. Eroms, R. Yakimova, S. Lara-Avila,

- S. Kubatkin, and S. D. Ganichev, *Phys. Rev. Lett.* **105**, 227402 (2010).
- ¹⁶E. McCann, K. Kechedzhi, V. I. Fal'ko, H. Suzuura, T. Ando, and B. L. Altshuler, *Phys. Rev. Lett.* **97**, 146805 (2006).
- ¹⁷D. N. Mirlin, in *Optical Orientation*, edited by F. Meier and B. P. Zakharchenya (Elsevier Science, Amsterdam, 1984).
- ¹⁸D. M. Basko, S. Piscanec, and A. C. Ferrari, *Phys. Rev. B* **80**, 165413 (2009).
- ¹⁹E. G. Mishchenko, *Phys. Rev. Lett.* **98**, 216801 (2007).
- ²⁰D. C. Elias, R. V. Gorbachev, A. S. Mayorov, S. V. Morozov, A. A. Zhukov, P. Blake, K. S. Novoselov, A. K. Geim, and F. Guinea, *Nat. Phys.* **7**, 701 (2011).
- ²¹F. Guinea, M. I. Katsnelson, and A. K. Geim, *Nat. Phys.* **6**, 30 (2010).